the tube was stored in a refrigerator (-25 °C) for 2 weeks. After decanting of the solvent, the crystals were washed with diethyl ether.

A small prismatic crystal was mounted at a random orientation on a glass fiber for both space group and cell constant determination. The data were collected using a Nonius CAD4 diffractometer. Cell constants were obtained by least-square fit of 25 high-angle reflections ($9.9 < \theta < 17.2$) using the CAD4 centering routines.

Crystallographic and experimental data are listed in Table VI and in the supplementary material, Table S1. Three reflections were chosen as standards to check the decay of the crystal and the stability of the experimental conditions and measured every 1 h; the crystal orientation was checked by measuring three standards every 300 reflections. No significant variation was observed.

Data were collected at variable scan speeds to ensure constant statistical precision of the measured intensities. A total of 5125 reflections ($\pm h, \pm k, +l$) were measured and corrected for Lorentz and polarization factors.[23] An absorption correction was then calculated using the ψ scans of five reflections at high χ angles ($\chi > 84°$). A total of 4254 reflections were considered as observed having $F_o^2 \geq 2.0\sigma(F^2)$, while $F_o^2 = 0.0$ was given to those reflections having negative net intensities.

The structure was solved by standard Patterson and Fourier methods and refined by full-matrix least square minimizing the function $\sum(w(F_o - 1/kF_c)^2)$. An isotropic extinction parameter was refined but found to be negligible and not considered in the final refinement. The scattering factors used, corrected for the anomalous dispersion,[24] were taken from tabulated values.[24] Anisotropic temperature parameters were used for all atoms, and the contribution of the hydrogen atoms, held fixed at their calculated positions (C-H = 0.95 Å, B_{iso} = 5.0 Å^2), was also taken into account but not refined. Upon convergence a Fourier difference map showed no significant features. All calculations were carried out using the Nonius SDP package.[25] Final positional parameters are listed in Table VII.

Acknowledgment. B.S. carried out work during the tenure of a fellowship from the Swiss National Foundation.

Registry No. **1**, 82884-19-3; **2a**, 17522-96-2; **2b**, 94992-93-5; **2c**, 59599-36-9; **2d**, 17522-93-9; **2e**, 15282-39-0; **2f**, 136984-68-4; [**3a**][**4a**], 136953-68-9; [**3b**][**4b**], 136953-70-3; [**3c**][**4c**], 136953-72-5; [**3d**][**4d**], 136953-74-7; [**3e**][**4e**], 136953-76-9; [**4a**][**5a**], 136984-63-9; [**4a**][**9a**], 136953-86-1; [**4b**][**5b**], 136953-78-1; [**4b**][**9b**], 136953-88-3; [**4c**][**5c**], 136953-80-5; [**4c**][**9c**], 136953-90-7; [**4d**][**5d**], 136953-82-7; [**4d**][**9d**], 136953-92-9; [**4d**][**13**], 136953-96-3; [**4d**][**14**], 137036-74-9; [**4d**][**15**], 136953-98-5; [**4d**][**16**], 136954-00-2; [**4d**][**17**], 136954-02-4; [**4e**][**5e**], 136953-84-9; [**4e**][**9e**], 136953-94-1; [**4f**][**9f**], 136984-44-6; **6d**, 17522-86-0; [**7d**][**8d**], 136984-65-1; [**8d**][**10d**], 136954-05-7; [**13**][SbF_6], 136954-03-5; [**18**][SbF_6], 136984-67-3; **19d**, 136954-06-8; PhSH, 108-98-5; H_2O, 7732-18-5; 1-thio-1-phenyl-2-(2-pyridyl)-4,5-dimethyl-1-phospha-2,4-cyclohexadiene, 82884-21-7.

Supplementary Material Available: Tables of X-ray experimental data (Table S1) and anisotropic thermal parameters (Table S2) and an extended list of bond lengths and angles (Table S3) (6 pages); a table of observed and calculated structure factors (Table S4) (43 pages). Ordering information is given on any current masthead page.

Contribution from the Department of Inorganic and Physical Chemistry, Indian Institute of Science, Bangalore 560 012, India

Nucleophilic Attacks of 1,2-Diaminoethane on MeCN Ligands: Synthesis, X-ray Structure, and Spectral and Electrochemical Properties of $[Ru_2(\mu\text{-}O)(\mu\text{-}O_2CAr)_2\{NH_2CH_2CH_2NHC(Me)NH\}_2(PPh_3)_2](ClO_4)_2$ (Ar = C_6H_4-*p*-X; X = H, Me, OMe, Cl)

Ariyanchira Syamala and Akhil R. Chakravarty*

Received February 5, 1991

The diruthenium(III) complex $[Ru_2O(O_2CAr)_2(MeCN)_4(PPh_3)_2](ClO_4)_2$ (**1**), on reaction with 1,2-diaminoethane (en) in MeOH at 25 °C, undergoes nucleophilic attacks at the carbon of two facial MeCN ligands to form $[Ru_2^{III}O(O_2CAr)_2\{NH_2CH_2CH_2NHC(Me)NH\}_2(PPh_3)_2](ClO_4)_2$ (**2**) (Ar = C_6H_4-*p*-X, X = H, Me, OMe, Cl) containing two seven-membered amino-amidine chelating ligands. The molecular structure of **2** with Ar = C_6H_4-*p*-OMe was determined by X-ray crystallography. Crystal data are as follows: triclinic, $P\bar{1}$, a = 13.942 (5) Å, b = 14.528 (2) Å, c = 21.758 (6) Å, α = 109.50 (2)°, β = 92.52 (3)°, γ = 112.61 (2)°, V = 3759 (2) Å^3, and Z = 2. The complex has an $\{Ru_2(\mu\text{-}O)(\mu\text{-}O_2CAr)_2^{2+}\}$ core. The Ru-Ru and average Ru-O_{oxo} distances and the Ru-O-Ru angle are 3.280 (2) Å, 1.887 [8] Å, and 120.7 (4)°, respectively. The amino group of the chelating ligand is trans to the μ-oxo ligand. The nucleophilic attacks take place on the MeCN ligands cis to the μ-oxo ligand. The visible spectra of **2** in $CHCl_3$ display an absorption band at 565 nm. The ^{1}H NMR spectra of **2** in $CDCl_3$ are indicative of the formation of an amino-amidine ligand. Complex **2** exhibits metal-centered quasireversible one-electron oxidation and reduction processes in the potential ranges +0.9 to +1.0 V and -0.3 to -0.5 V (vs SCE), respectively, involving the $Ru^{III}_2/Ru^{III}Ru^{IV}$ and $Ru^{III}_2/Ru^{II}Ru^{III}$ redox couples in CH_2Cl_2 containing 0.1 M TBAP. The mechanistic aspects of the nucleophilic reaction are discussed.

Introduction

The discovery[1] of a (μ-oxo)bis(μ-carboxylato)diiron core in the active sites of a number of non-heme metalloproteins has generated considerable current interest[2-4] in the synthesis of low molecular weight transition-metal complexes with a similar core structure. The role of facial as well as bridging ligands in tuning and controlling the electronic structure of the dimetallic core is an interesting aspect of this chemistry. It is a general observation that

(1) Stenkamp, R. E.; Sieker, L. C.; Jensen, L. H.; McCallum, J. D.; Sanders-Loehr, J. *Proc. Natl. Acad. Sci. U.S.A* **1985**, *82*, 713. Stenkamp, R. E.; Sieker, L. C.; Jensen, L. H.; Sanders-Loehr, J. *Nature (London)* **1981**, *291*, 263. Stenkamp, R. E.; Sieker, L. C.; Jensen, L. H. *J. Am. Chem. Soc.* **1984**, *105*, 618. Klotz, I. M.; Kurtz, D. M., Jr. *Acc. Chem. Res.* **1984**, *17*, 16. Nordlund, P.; Sjöberg, B.-M.; Eklund, H. *Nature (London)* **1990**, *345*, 593. Reichard, P.; Ehrenberg, A. *Science* **1983**, *221*, 514. Lynch, J. B.; Juarez-Garcia, C.; Münck, E.; Que, L., Jr. *J. Biol. Chem.* **1989**, *264*, 8091.

(2) Lippard, S. J. *Angew. Chem., Int. Ed. Engl.* **1988**, *27*, 344.

(3) Wilkins, P. C.; Wilkins, R. G. *Coord. Chem. Rev.* **1987**, *79*, 195. Wilkins, R. G.; Harrington, P. C. *Adv. Inorg. Biochem.* **1983**, *5*, 51. Sanders-Loehr, J.; Wheeler, W. D.; Shiemke, A. K.; Averill, B. A.; Loehr, T. M. *J. Am. Chem. Soc.* **1989**, *111*, 8084. Reem, R. C.; McCormick, J. M.; Richardson, D. E.; Devlin, F. J.; Stephens, P. J.; Musselman, R. J.; Solomon, E. I. *J. Am. Chem. Soc.* **1989**, *111*, 4688.

(4) Kurtz, D. M., Jr. *Chem. Rev.* **1990**, *90*, 585. Wieghardt, K. *Frontiers in Bioinorganic Chemistry*; Xavier, A. V., Ed.; VCH Publishers: Weinheim, West Germany, 1986; pp 246-255.

0020-1669/91/1330-4699$02.50/0

the metal oxidation state in the core is predominantly +3 although analogous cores containing metals in other oxidation states are also reported.[2,5,6]

Considering the chemical relevance of the model complexes to the hemerythrin biomolecules, the major thrust was on the synthesis and characterization of diiron complexes.[2-4,7] Recent developments in this chemistry have shown that besides other 3d elements,[2,8] the dimeric core can be stabilized as well by a 4d element, viz., ruthenium.[6,9-12] The complexes reported are of the type $[\{(L)Ru^{III}\}_2(\mu\text{-}O)(\mu\text{-}O_2CMe)_2]X_2$, where L = 1,4,7-trimethyl-1,4,7-triazacyclononane (Me_3tacn),[6] tripyrazolylmethane (tpm),[10] or three unidentate pyridine[9] ligands and X = PF_6^- or ClO_4^-. These complexes have substitutionally inert facial ligands. The other known[11,12] diruthenium complexes are $[Ru_2O(O_2CMe)_4(PPh_3)_2]$, $[Ru_2O(O_2CAr)_4(PPh_3)_2]$, and $[Ru_2O(O_2CAr)_2(MeCN)_4(PPh_3)_2](ClO_4)_2$ (**1**) (Ar = aryl group). The presence of labile facial carboxylato and MeCN ligands makes these complexes suitable for further studies aimed at the facial sites of the diruthenium core.

As a part of our systematic investigations[11] on (μ-oxo)diruthenium complexes, the present work stems from our interest in studying the reactivity of **1** toward 1,2-diaminoethane (en). The product obtained from a reaction of **1** with en is a novel complex of the type $[Ru_2O(O_2CAr)_2\{NH_2CH_2CH_2NHC(Me)NH\}_2(PPh_3)_2](ClO_4)_2$ (**2**), which is presumably formed by nucleophilic attacks of en on the carbon atoms of two facial MeCN ligands in **1**. The reaction demonstrates the electron-withdrawing ability of the strongly coupled $\{Ru_2(\mu\text{-}O)^{4+}\}$ core in triply bridged diruthenium(III) complexes. Herein we report the synthesis, spectral properties, and electrochemical behavior of **2** [Ar = C_6H_4-*p*-X; X = H (**2a**), Me (**2b**), OMe (**2c**), and Cl (**2d**)]. Complex **2c** has been characterized by X-ray studies.

Experimental Section

Materials and Methods. The solvents and reagents, purchased from commercial sources, were used without further purification. Dichloromethane and chloroform used for cyclic voltammetric and visible spectral studies were purified by conventional methods.

Synthesis of $Ru_2Cl(O_2CMe)_4$ from $RuCl_3{\cdot}3H_2O$ and its conversion to $Ru_2Cl(O_2CAr)_4$ were carried out by following reported[12,13] procedures. $Ru_2Cl(O_2CAr)_4$ was reacted with PPh_3 to prepare the purple complexes $Ru_2O(O_2CAr)_4(PPh_3)_2$ (Ar = C_6H_4-*p*-X; X = H, Me, OMe, Cl) by following a procedure that we have published[11] earlier. This complex was converted[11] quantitatively to the blue precursor complex $Ru_2O(O_2CAr)_2(MeCN)_4(PPh_3)_2(ClO_4)_2$ (**1**) [Ar = C_6H_4-*p*-X; X = H, (**1a**), Me (**1b**), OMe (**1c**), Cl (**1d**)] by dissolving $Ru_2O(O_2CAr)_4(PPh_3)_2$ in MeCN containing the calculated amount of $HClO_4$. Characterization of **1** was done by elemental analysis and by visible and ^1H NMR spectroscopic methods.

Safety Note. Perchlorate salts of metal complexes with organic ligands are potentially explosive. Only small amounts of material should be prepared, and these should be handled with great caution.

Preparation of $[Ru_2O(O_2CAr)_2\{NH_2CH_2CH_2NHC(Me)NH\}_2(PPh_3)_2](ClO_4)_2$ [Ar = C_6H_4-*p*-X; X = H (2a), Me (2b), OMe (2c), Cl (2d)]. Complexes **2a–d** were prepared by following a general synthetic procedure. A representative one is given below.

Complex **2c** was prepared by stirring a 0.30 g (0.2 mmol) of **1c** with 0.08 g (1.2 mmol) of 1,2-diaminoethane (en) in 6 mL of methanol for 12 h at 25 °C. The blue precipitate thus obtained was filtered,[14] washed with cold H_2O–MeOH mixture (1:4 v/v) and dried in vacuo over P_4O_{10}. The crude product was then recrystallized from a CH_2Cl_2–*n*-hexane mixture. Yield: 0.06 g (ca. 19%).[14] Anal. Calcd for $C_{60}H_{66}N_6O_{15}P_2Cl_2Ru_2$: C, 49.80; H, 4.60; N, 5.81. Found: C, 49.17; H, 4.75; N, 6.10. Visible spectral data in $CHCl_3$ (λ_{max}): 565 (ϵ, 8500 M^{-1} cm^{-1}), 379 nm (sh). Characterization data for complex **2a** are as follows. Yield: ca. 9%. Anal. Calcd for $C_{58}H_{62}N_6O_{13}P_2Cl_2Ru_2$: C, 50.25; H, 4.50; N, 6.06. Found: C, 49.20; H, 4.50; N, 6.81. λ_{max}: 565 (ϵ, 8800 M^{-1} cm^{-1}), 379 nm (sh). Characterization data for complex **2b** are as follows. Yield: ca. 10%. Anal. Calcd for $C_{60}H_{66}N_6O_{13}P_2Cl_2Ru_2$: C, 50.95; H, 4.71; N, 5.90. Found: C, 50.08; H, 4.99; N, 6.18. λ_{max}: 565 (ϵ, 8400 M^{-1} cm^{-1}), 379 nm (sh). Characterization data for complex **2d** are as follows. Yield: ca. 17%. Anal. Calcd for $C_{58}H_{60}N_6O_{13}P_2Cl_4Ru_2$: C, 47.86; H, 4.16; N, 5.78. Found: C, 47.25; H, 4.05; N, 6.13. λ_{max}: 565 (ϵ, 7300 M^{-1} cm^{-1}), 379 nm (sh). Complex **2** was found to be soluble in Me_2CO, CH_2Cl_2, and $CHCl_3$, less soluble in MeCN and MeOH, and essentially insoluble in C_6H_6 and H_2O.

Measurements. The elemental analyses were made with a Heraeus CHN-O Rapid instrument. Visible absorption spectra were recorded with a Hitachi U-3400 spectrophotometer. The ^1H NMR spectra were obtained with Bruker WH-270 and AC(AF) 200-MHz spectrometers. Cyclic voltammetric measurements were done using a three-electrode setup on a PAR Model 174A polarographic analyzer connected with a Houston Instruments Omnigraphic X-Y recorder. A platinum button, a platinum wire, and a saturated calomel electrode were used as working, auxiliary and reference electrodes, respectively. Dichloromethane containing 0.1 M Bu_4NClO_4 (TBAP) as the supporting electrolyte was used as the solvent, and the measurements were made at 25 °C. The data were not corrected for junction potentials. Ferrocene, $(\eta^5\text{-}Cp)_2Fe$, was used as a standard to verify the potentials observed against the saturated calomel electrode (SCE) and to obtain the electron-transfer stoichiometries of the redox couples by peak current measurements. The Fe(II/III) couple of ferrocene was observed at +0.51 V (vs SCE) under similar experimental conditions in CH_2Cl_2 containing 0.1 M TBAP at 25 °C.

X-ray Crystallographic Procedures. Collection and Reduction of Data. Single crystals of **2c** were obtained by layering a CH_2Cl_2 solution of **2c** with *n*-hexane in a Schlenk tube. The crystals turned to powder on removal from the mother liquor, so a rectangular shaped crystal was sealed in a Lindemann capillary along with the mother liquor. Unit cell parameters were obtained from this crystal mounted on an Enraf-Nonius CAD4 four-circle diffractometer by a least-squares fit of 25 reflections with $24° < 2\theta < 36°$. The triclinic crystal of **2c** was found to belong in the space group $P\bar{1}$, which was subsequently confirmed by successful solution and refinement of the structure. The unit cell parameters and information related to intensity data collection are summarized in Table I. Intensity data were corrected for Lorentz, polarization, and absorption effects.[15a]

Table I. Crystallographic Data for $[Ru_2O(O_2CC_6H_4\text{-}p\text{-}OMe)_2\{NH_2CH_2CH_2NHC(Me)NH\}_2(PPh_3)_2](ClO_4)_2{\cdot}CH_2Cl_2{\cdot}1.5H_2O$ (**2c**)

chem formula	$C_{61}H_{71}N_6O_{16.5}P_2Cl_4Ru_2$	V, Å^3	3759 (2)
fw	1558.16	Z	2
space group	$P\bar{1}$ (No 2)	ρ_{calcd}, g cm^{-3}	1.38
a, Å	13.942 (5)	μ, cm^{-1}	6.39
b, Å	14.528 (2)	λ, Å (Mo–Kα)	0.7107
c, Å	21.758 (6)	T, °C	17
α, deg	109.50 (2)	transm coeff	0.95–1.09[a]
β, deg	92.52 (3)	R^b	0.0853
γ, deg	112.61 (2)	R_w^c	0.0931

[a] Normalized to an average of unity. [b] $R = \sum(|F_o| - |F_c|)/\sum|F_o|$. [c] $R_w = [\sum w(|F_o| - |F_c|)^2/\sum w|F_o|^2]^{1/2}$; $w = k/[\sigma^2(F_o) + gF_o^2]$.

(5) Armstrong, J. E.; Robinson, W. R.; Walton, R. A. *Inorg. Chem.* **1983**, *22*, 1301.
(6) Neubold, P.; Wieghardt, K.; Nuber, B.; Weiss, J. *Inorg. Chem.* **1989**, *28*, 459.
(7) Norman, R. E.; Holz, R. C.; Ménage, S.; O'Connor, C. J.; Zhang, J. H.; Que, L., Jr. *Inorg. Chem.* **1990**, *29*, 4629. Adams, H.; Bailey, N. A.; Crane, J. D.; Fenton, D. E.; Latour, J. H.; Wiliams, J. M. *J. Chem. Soc., Dalton Trans.* **1990**, 1727. Beer, R. H.; Tolman, W. B.; Bott, S. G.; Lippard, S. J. *Inorg. Chem.* **1989**, *28*, 4557. Drüeke, S.; Wieghardt, K.; Nuber, B.; Weiss, J.; Fleischhauer, H. P.; Gehring, S.; Haase, W. *J. Am. Chem. Soc.* **1989**, *111*, 8622. Tolman, W. B.; Bino, A.; Lippard, S. J. *J. Am. Chem. Soc.* **1989**, *111*, 8522. Feng, X.; Bott, S. G.; Lippard, S. J. *J. Am. Chem. Soc.* **1989**, *111* 8046. Wu, F. J.; Kurtz, D. M., Jr. *J. Am. Chem. Soc.* **1989**, *111*, 6563. Drüeke, S.; Wieghardt, K.; Nuber, B.; Weiss, J. *Inorg. Chem.* **1989**, *28*, 1414.
(8) Gafford, B. G.; Marsh, R. E.; Schaefer, W. P.; Zhang, J. H.; O'Connor, C. J.; Holwerda, R. A. *Inorg. Chem.* **1990**, *29*, 4652. Bodner, A.; Drüeke, S.; Wieghardt, K.; Nuber, B.; Weiss, J. *Angew. Chem., Int. Ed. Engl.* **1990**, *29*, 68. Bossek, U.; Wieghardt, K.; Nuber, B.; Weiss, J. *Inorg. Chim. Acta* **1989**, *165*, 123. Bossek, U.; Weyhermuller, T.; Wieghardt, K.; Bonvoisin, J.; Girerd, J. J. *J. Chem. Soc., Chem. Commun.* **1989**, 633.
(9) Sasaki, Y.; Suzuki, M.; Tokiwa, A.; Ebihara, M.; Yamaguchi, T.; Kabuto, C.; Ito, T. *J. Am. Chem. Soc.* **1988**, *110*, 6251.
(10) Llobet, A.; Curry, M. E.; Evans, H. T.; Meyer, T. J. *Inorg. Chem.* **1989**, *28*, 3131.
(11) Das, B. K.; Chakravarty, A. R. *Inorg. Chem.* **1990**, *29*, 2078.
(12) Mitchell, R. W.; Spencer, A.; Wilkinson, G. *J. Chem. Soc., Dalton Trans.* **1973**, 846.
(13) Das, B. K.; Chakravarty, A. R. *Polyhedron* **1988**, *7*, 685.

(14) The filtrate color was yellow. The yield of **2** is low since the major product of this reaction is an uncharacterized yellow complex, which is under investigation. Detailed report on this complex will be made elsewhere.

Structure Solution and Refinement. The structure was solved by the Patterson heavy-atom method using the SHELXS-86 program[15b] on the DEC-1090 and VAX-8810 computer systems at the Indian Institute of Science. Atom peaks not appearing in this way were found by successive structure factor–difference Fourier calculations using the SHELX-76 program,[15b] which was also used for refining the structures by full-matrix least-squares methods. One phenyl group bonded to P(1) was found to be disordered. The atoms C41–C46 and C91–C96 were refined as rigid groups with a site occupancy factor of 0.5. The hydrogens in the complex, excluding the NH_2 and the disordered phenyl groups, were put in the calculated positions for calculation of structure factors. Except for the carbon atoms C41–C46 and C91–C96 in the disordered phenyl groups, the CH_2Cl_2 solvent, and the oxygen atoms of the solvent water molecules, all other atoms were refined anisotropically. The source of water molecules in the crystal structure could be the solvents used for crystallization of **2c**. The oxygen atoms of the ClO_4^- groups were found to be disordered. The least-squares refinement converged to R indices listed in Table I.

Disorder and Other Difficulties. Crystals of **2c** were found to be soft. The volatile mother liquor, a mixture of CH_2Cl_2 and n-hexane, posed a problem. The movement of the crystal in the capillary necessitated recentering of the crystal during data collection. Besides this, the solvent molecules, the phenyl group carbons (C41–C46, C91–C96), and the perchlorate oxygens were found to be in a highly disordered state and showed relatively high thermal parameters. Even though these disordered moieties were modeled as best as possible in the usual manner, all the above-mentioned factors combined together probably contributed to the higher values of the R indices. As a whole the structure does not show any chemically or crystallographically suspicious features.

Results

Synthesis. Earlier we have shown[11] that the metal–metal multiple bonded diruthenium(II,III) complex $Ru_2Cl(O_2CAr)_4$, on reaction with PPh_3 in MeCN, undergoes a facile core conversion leading to the formation of diruthenium(III) complexes $Ru_2O(O_2CAr)_4(PPh_3)_2$ and $Ru_2O(O_2CAr)_2(MeCN)_4(PPh_3)_2(ClO_4)_2$ (**1**). In MeCN, $Ru_2O(O_2CAr)_4(PPh_3)_2$ converts quantitatively to **1** on addition of $HClO_4$. Complex **1** containing two labile MeCN facial ligands on each metal center is chosen as a precursor to study the reactivity of the bidentate chelating ligand 1,2-diaminoethane (en) with the dimeric core in **1**.

Complex **1** was found to react smoothly with en under mild reaction conditions to form a blue species **2** and a methanol-soluble yellow species.[14] Complex **2** was initially formulated as $[Ru_2O(O_2CAr)_2(MeCN)_2(en)_2(PPh_3)_2](ClO_4)_2$ from the elemental analysis and the ^1H NMR spectral data. From the X-ray crystallographic studies it was reformulated as $[Ru_2O(O_2CAr)_2\{NH_2CH_2CH_2NHC(Me)NH\}_2(PPh_3)_2](ClO_4)_2$ (**2**). The MeCN facial ligands in **1** are thus susceptible to nucleophilic attacks at carbon by en to form an amino–amidine ligand, $NH_2CH_2CH_2NHC(Me)NH$, which is stabilized on chelate formation with the metal center. Similar sorts of nucleophilic reactions (eqs 1 and 2) leading to the formation of amides and

$$\{M{-}N{\equiv}C{-}R\}^{n+} + OH^- \rightarrow \{M{-}NH{-}C(=O)R\}^{(n-1)+} \quad (1)$$

$$\{M{-}N{\equiv}C{-}R\}^{n+} + R'NH_2 \rightarrow \{M{-}NH{=}C(R)NHR'\}^{n+} \quad (2)$$

amidines are known[16-18] in monomeric complexes. Bidentate ligands with one or two amine functionalities can form a seven-membered chelate as is reported[18] in the platinum(II) complex, $[PtCl(NHCOPh)\{NH{=}C(Ph)N(t\text{-}Bu)CH_2CH_2N(t\text{-}Bu)H\}]$.

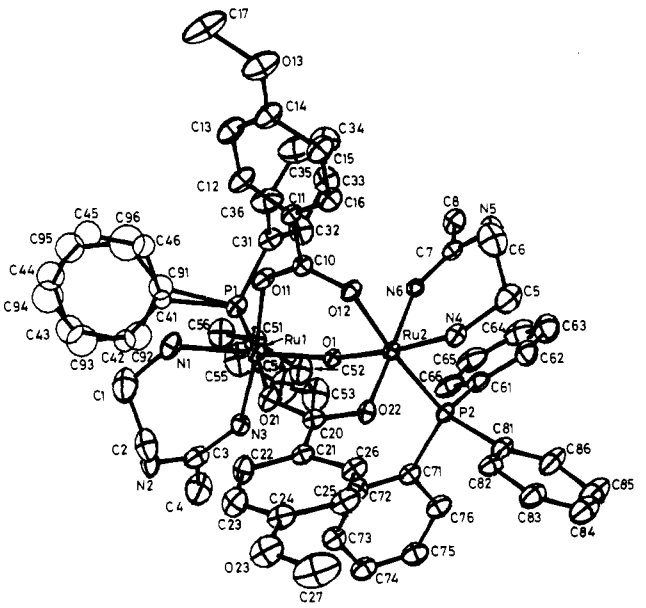

Figure 1. ORTEP view of $[Ru_2O(O_2CC_6H_4\text{-}p\text{-}OMe)_2\{NH_2CH_2CH_2NHC(Me)NH\}_2(PPh_3)_2]^{2+}$ showing the 20% probability thermal ellipsoids and atomic labeling scheme. Atoms C41–C46 and C91–C96 belong to the disordered phenyl groups.

Table II. Fractional Atomic Coordinates ($\times 10^4$)[a] and Isotropic Thermal Parameters ($\times 10^3$) for Selected Atoms with Their Estimated Standard Deviations for $[Ru_2O(O_2CC_6H_4\text{-}p\text{-}OMe)_2\{NH_2CH_2CH_2NHC(Me)NH\}_2(PPh_3)_2](ClO_4)_2\cdot CH_2Cl_2\cdot 1.5H_2O$ (**2c**)

atom	x/a	y/b	z/c	U_{eq},[b] Å^2
Ru1	765 (1)	1576 (1)	3052 (0.3)	40 (0.3)
Ru2	2880 (1)	2063 (1)	2385 (0.3)	39 (0.3)
O1	1717 (5)	2354 (5)	2618 (3)	41 (3)
P1	621 (2)	3114 (2)	3700 (1)	53 (1)
P2	2783 (2)	2465 (2)	1451 (1)	43 (1)
O11	1889 (6)	1753 (6)	3784 (3)	57 (4)
O12	3163 (5)	1652 (6)	3202 (3)	52 (3)
O22	2074 (5)	441 (5)	1864 (3)	49 (3)
O21	805 (6)	59 (5)	2477 (3)	54 (3)
N1	−227 (8)	559 (8)	3541 (5)	73 (5)
N2	−2115 (8)	−57 (10)	2389 (7)	87 (6)
N3	−491 (6)	1317 (7)	2376 (5)	60 (5)
N4	4222 (7)	1681 (7)	2219 (4)	56 (4)
N5	5570 (9)	4339 (9)	3162 (7)	93 (6)
N6	3730 (6)	3682 (6)	2966 (4)	50 (4)
C1	−1273 (14)	−226 (15)	3322 (12)	129 (12)
C2	−1686 (12)	−691 (12)	2596 (11)	103 (9)
C3	−1565 (10)	764 (12)	2235 (6)	75 (8)
C4	−2180 (11)	1187 (15)	1878 (8)	104 (11)
C5	5299 (12)	2488 (14)	2341 (8)	96 (10)
C6	5612 (12)	3227 (17)	3084 (10)	111 (11)
C7	4673 (9)	4466 (8)	3177 (5)	57 (5)
C8	4849 (11)	5595 (10)	3492 (6)	78 (6)
C10	2743 (8)	1664 (8)	3707 (5)	46 (5)
C20	1332 (7)	−191 (7)	2055 (5)	45 (4)
C31	1872 (10)	4201 (9)	4287 (6)	70 (6)
C51	197 (9)	3791 (8)	3251 (7)	73 (6)
C61	3362 (9)	3906 (8)	1624 (5)	65 (5)
C71	1459 (8)	1964 (8)	962 (5)	52 (5)
C81	3362 (8)	1814 (10)	798 (4)	60 (6)
C41	−459 (15)	2812 (14)	4172 (10)	47 (5)
C91	−309 (16)	2840 (19)	4309 (18)	86 (8)

[a] The atoms C41 and C91 are refined with a site occupancy factor (sof) of 0.5. [b] $U_{iso}(eq) = [\sum_i\sum_j U_{ij}a_i^*a_j^*a_ia_j]/3$.

Molecular Structure. The cation of **2c**, shown in Figure 1, consists of a diruthenium(III) unit held by an oxo bridge and two bridging arenecarboxylato ligands in a cis disposition forming an $\{Ru_2(\mu\text{-}O)(\mu\text{-}O_2CAr)_2^{2+}\}$ core that is analogous to the core in complex **1**. The geometry around the metal centers is nearly

(15) (a) North, A. C. T.; Phillips, D. C.; Mathews, F. S. *Acta Crystallogr.* **1968**, *A24*, 351. (b) Sheldrick, G. M. SHELXS-86. A Computer Program for Automatic Solution of Crystal Structures. Universität Göttingen, 1986. Sheldrick, G. M. *A Program for Crystal Structure Determination*; Cambridge University Press: Cambridge, England, 1976.

(16) Storhoff, B. N.; Lewis, H. C., Jr. *Coord. Chem. Rev.* **1977**, *23*, 1. Cotton, F. A.; Wilkinson, G. *Advanced Inorganic Chemistry*, 5th ed.; John Wiley & Sons: New York, 1988; p 361.

(17) Paul, P.; Nag, K. *Inorg. Chem.* **1987**, *26*, 1586. Anderes, B.; Lavallee, D. K. *Inorg. Chem.* **1983**, *22*, 3724. Thorn, D. L.; Calabrese, J. C. *J. Organomet. Chem.* **1984**, *272*, 283. Buckingham, D. A.; Clark, C. R.; Foxman, B. M.; Gainsford, G. J.; Sargeson, A. M.; Wein, M.; Zanella, A. *Inorg. Chem.* **1982**, *21*, 1986.

(18) Maresca, L.; Natile, G.; Intini, F. P.; Gasparrini, F.; Tiripicchio, A.; Tiripicchio-Camellini, M. *J. Am. Chem. Soc.* **1986**, *108*, 1180.

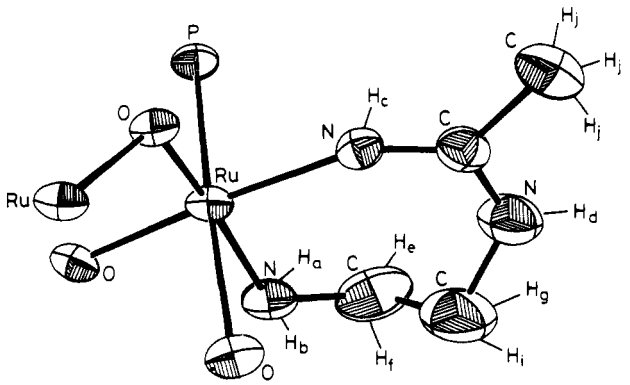

Figure 2. Coordination around one ruthenium(III) atom in **2** showing the amino–amidine seven-membered chelate ring.

octahedral, but the conformation of the molecule is essentially staggered. An ORTEP[19] view of the coordination sphere is presented in Figure 2. The facial ligands on each metal center are one PPh_3 and one amino–amidine ligand, $NH_2CH_2CH_2NHC(Me)NH$, forming a seven-membered metallacycle (Figure 2).

Selected atomic coordinates and isotropic thermal parameters of **2c** are given in Table II. Table III lists selected bond distances and angles in **2c**. The Ru1–Ru2 distance of 3.280 (2) Å in **2c** is considerably longer than the 3.237 (1) and 3.199 (1) Å values observed[11] for that in **1** and $Ru_2O(O_2CAr)_4(PPh_3)_2$, respectively. The Ru–O–Ru angle is 120.7 (4)° in **2c**. The Ru–O_{oxo} distance of 1.887 (8) Å is comparable with that in other reported[6,9-11] (μ-oxo)diruthenium(III) complexes. Such a short Ru–O distance indicates the presence of a strong interaction between two t_{2g}^5 Ru(III) centers through the μ-oxo ligand. The π-acceptor ability of the PPh_3 ligand is reflected in the longer Ru1–O21, Ru2–O12 distances of ca. 2.14 Å compared to the Ru1–O11 and Ru2–O22 bond lengths of ca. 2.05 Å. Due to the steric bulk of the PPh_3 ligand, the P–Ru–O and P–Ru–N angles are obtuse.

The amino group of the chelating facial ligand is trans to the μ-oxo ligand (Figure 2). The Ru–N(amino) distance of 2.18 Å is considerably longer than the Ru–N(amidine) bond length of 2.07 Å. This trans effect is related to the shorter Ru–O bonds in the $\{Ru_2(\mu\text{-}O)^{4+}\}$ moiety. The molecular structure of **2c** shows that the MeCN ligands cis to the μ-oxo ligand in **1** undergo nucleophilic attacks.

In the chelate ring, the N2–C3 and N5–C7 distances are similar to the N3–C3 and N6–C7 bond lengths due to the presence of two resonating structures involving this moiety. Again the shortening of the N2–C3 and N5–C7 distances compared to the N2–C2 and N5–C6 distances also suggests the significant contribution of both of the resonating forms, $NH_2CH_2CH_2NHC(Me)=NH \leftrightarrow NH_2CH_2CH_2NH=C(Me)NH$, in the chelate ring. The acute N1–Ru1–O11,O21 and N4–Ru2–O12,O22 angles of ca. 80° could be due to steric constraints imposed on the seven-membered chelate ring by the bulky PPh_3 facial ligand.

Spectral Properties. The visible spectra of **2** in $CHCl_3$ exhibit a strong absorption band at 565 nm with a molar extinction coefficient of ca. 8000 M^{-1} cm^{-1}. A representative spectrum is shown in Figure 3. The origin of this band is believed to be charge transfer in nature involving the Ru(III)–dπ and μ-O–pπ orbitals and is similar to those observed[6,9-12] in other (μ-oxo)diruthenium(III) complexes. It is observed that the substituents on the bridging arenecarboxylato ligands have no effect on this transition. The band position is, however, found to be sensitive to the type of facial ligands. Complex **1** and $Ru_2O(O_2CAr)_4(PPh_3)_2$ are known[11] to display equally intense bands at 581 and 562 nm, respectively. The energy of the CT band thus follows the order $ArCO_2^- > NH_2CH_2CH_2NHC(Me)NH > 2MeCN$ for **1**, **2**, and $Ru_2O(O_2CAr)_4(PPh_3)_2$. Since a PPh_3 ligand is present as a facial ligand on each metal center in these complexes, the π-acidity effect of the ligand(s) occupying the remaining facial sites on the low-energy absorption is evidenced from the visible spectral data.

Table III. Selected Bond Distances (Å) and Angles (deg) for $[Ru_2O(O_2CC_6H_4\text{-}p\text{-}OMe)_2\{NH_2CH_2CH_2NHC(Me)NH\}_2(PPh_3)_2](ClO_4)_2\cdot CH_2Cl_2\cdot 1.5H_2O$ (**2c**)

(a) Bond Lengths

Ru1–Ru2	3.280 (2)	P2–C81	1.832 (12)
Ru1–O1	1.897 (7)	O11–C10	1.259 (15)
Ru2–O1	1.877 (8)	O12–C10	1.266 (13)
Ru1–P1	2.300 (3)	O22–C20	1.284 (12)
Ru1–O11	2.063 (8)	O21–C20	1.248 (13)
Ru1–O21	2.165 (7)	N1–C1	1.397 (18)
Ru1–N1	2.199 (12)	C1–C2	1.481 (32)
Ru1–N3	2.066 (10)	C2–N2	1.444 (28)
Ru2–P2	2.306 (3)	N2–C3	1.307 (22)
Ru2–O12	2.121 (8)	C3–C4	1.543 (30)
Ru2–O22	2.042 (6)	C3–N3	1.361 (14)
Ru2–N4	2.160 (11)	N4–C5	1.450 (16)
Ru2–N6	2.068 (7)	C5–C6	1.541 (24)
P1–C31	1.873 (10)	C7–C8	1.465 (18)
P1–C51	1.819 (16)	C7–N6	1.297 (11)
P1–C41	1.856 (22)	P2–C61	1.823 (11)
P1–C91	1.924 (34)	P2–C71	1.830 (11)

(b) Bond Angles

Ru1–O1–Ru2	120.7 (4)	Ru1–P1–C91	111.4 (9)
N1–Ru1–N3	94.8 (4)	Ru1–P1–C41	111.6 (7)
O21–Ru1–N3	93.0 (4)	Ru1–P1–C51	115.7 (5)
O21–Ru1–N1	80.4 (4)	Ru1–P1–C31	114.9 (5)
O11–Ru1–N3	173.3 (4)	Ru2–P2–C81	113.7 (4)
O11–Ru1–N1	78.7 (4)	Ru2–P2–C71	116.9 (4)
O11–Ru1–O21	87.3 (3)	Ru2–P2–C61	113.8 (3)
P1–Ru1–N3	86.6 (3)	Ru1–O11–C10	126.3 (6)
P1–Ru1–N1	95.1 (3)	Ru2–O12–C10	132.4 (8)
P1–Ru1–O21	175.5 (2)	Ru2–O22–C20	124.1 (6)
P1–Ru1–O11	92.6 (2)	Ru1–O21–C20	132.8 (7)
O1–Ru1–N3	89.4 (4)	O11–C10–O12	125.9 (10)
O1–Ru1–N1	173.1 (4)	O22–C20–O21	127.7 (10)
O1–Ru1–O21	94.0 (3)	Ru1–N1–C1	129.9 (12)
O1–Ru1–O11	97.2 (3)	N1–C1–C2	116.1 (17)
O1–Ru1–P1	90.6 (2)	C1–C2–N2	112.4 (17)
N4–Ru2–N6	97.1 (4)	C2–N2–C3	125.0 (14)
O22–Ru2–N6	176.1 (3)	N2–C3–N3	126.6 (14)
O22–Ru2–N4	81.5 (4)	N2–C3–C4	117.8 (14)
O12–Ru2–N6	90.4 (3)	C4–C3–N3	115.7 (14)
O12–Ru2–N4	76.6 (3)	Ru1–N3–C3	137.3 (9)
O12–Ru2–O22	85.7 (3)	Ru2–N4–C5	123.6 (10)
P2–Ru2–N6	90.5 (3)	N4–C5–C6	107.9 (14)
P2–Ru2–N4	95.0 (3)	C5–C6–N5	109.2 (15)
P2–Ru2–O22	93.4 (2)	C6–N5–C7	122.5 (13)
P2–Ru2–O12	171.6 (3)	N5–C7–N6	124.6 (12)
O1–Ru2–N6	83.0 (3)	N5–C7–C8	113.1 (12)
O1–Ru2–N4	173.3 (3)	C8–C7–N6	122.2 (12)
O1–Ru2–O22	98.0 (3)	Ru2–N6–C7	144.1 (8)
O1–Ru2–O12	96.6 (3)	O1–Ru2–P2	91.7 (2)

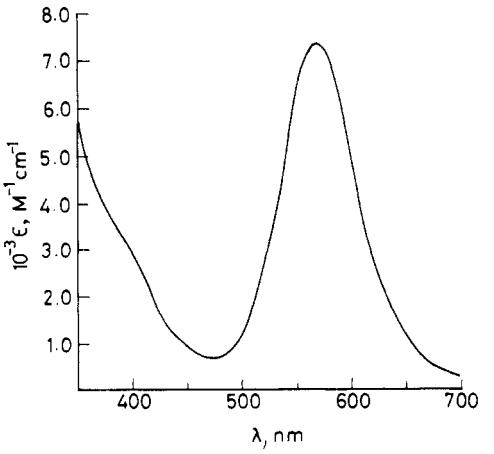

Figure 3. Visible absorption spectrum of $[Ru_2O(O_2CC_6H_4\text{-}p\text{-}Cl)_2\{NH_2CH_2CH_2NHC(Me)NH\}_2(PPh_3)_2](ClO_4)_2$ (**2d**) in $CHCl_3$.

(19) Johnson, C. K. ORTEP. Report ORNL-3794; Oak Ridge National Laboratory: Oak Ridge, TN, 1971.

Table IV. ^{1}H NMR Data[a] for $[Ru_2O(O_2CAr)_2\{NH_2CH_2CH_2NHC(Me)NH\}_2(PPh_3)_2](ClO_4)_2$ (**2**)

	δ, ppm				
complex	Me(chelate)[b]	Me(O_2CAr)[b]	$CH_2(H_{e-i})$[c]	NH_x (x = 1, 2)[d]	Ar, PPh_3[e]
2a (Ar = C_6H_5)	1.22 (6 H)		2.70 (2 H), 3.40 (2 H)	7.10 (4 H)	7.26–7.52 (m, 40 H)
			3.70 (2 H), 4.14 (2 H)	8.36 (2 H), 8.5 (2 H)	
2b (Ar = C_6H_4-*p*-Me)	1.19 (6 H)	2.33 (6 H)	2.63 (2 H), 3.39 (2 H)	7.15 (4 H)	7.09 (d, 4 H, J = 8)
			3.68 (2 H), 4.10 (2 H)	8.30 (4 H)	7.51 (d, 4 H, J = 5)
					7.27–7.37 (m, 30 H)
2c (Ar = C_6H_4-*p*-OMe)	1.18 (6 H)	3.78 (6 H)	2.65 (2 H), 3.40 (2 H)	6.92 (2 H)	6.78 (d, 4 H, J = 9)
			3.61 (2 H), 4.08 (2 H)	7.02 (2 H)	7.51 (d, 4 H, J = 5)
				8.18 (4 H)	7.26–7.44 (m, 30 H)
2d (Ar = C_6H_4-*p*-Cl)	1.22 (6 H)		2.63 (2 H), 3.41 (2 H)	7.11 (4 H)	7.27–7.77 (m, 38 H)
			3.62 (2 H), 4.15 (2 H)	8.62 (2 H)	
				8.85 (2 H)	

[a] $CDCl_3$, TMS as reference. [b] Singlet. [c] Multiplet. [d] Broad, undergoes exchange with D_2O. [e] Key: d, doublet; m, multiplet; J, Hz.

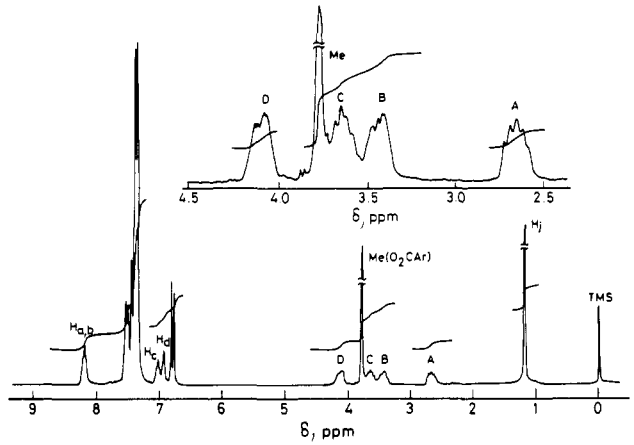

Figure 4. ^{1}H NMR spectrum of $[Ru_2O(O_2CC_6H_4$-*p*-$OMe)_2\{NH_2CH_2CH_2NHC(Me)NH\}_2(PPh_3)_2](ClO_4)_2$ (**2c**) in $CDCl_3$. The inset shows the multiplets of the CH_2 protons of the chelate ring.

^{1}H NMR spectra of **2** indicate the essentially diamagnetic nature of the complex. Relevant data are presented in Table IV and a representative spectrum is shown in Figure 4. Complex **2** exhibits a sharp singlet at δ 1.2 ppm for the methyl group protons (H_j) of the chelating ligands. Similarly, the methyl groups of two bridging carboxylato ligands in **2b** and **2c** appear as a sharp singlet. The spectral data thus show the equivalency of the metal centers in **2** in the solution phase. The observed nonequivalency of the metal centers in the solid-state X-ray structure could be due to crystal packing.

The chelate ring in **2**, shown in Figure 2, exhibits interesting spectral features. The H_a, H_b, and H_c protons are found to exchange with D_2O. The H_d proton also undergoes such an exchange with D_2O at 50 °C. The deshielding of the NH_2 (H_a, H_b) protons could be attributed to the trans effect of the $\{Ru_2(\mu\text{-}O)^{4+}\}$ moiety. The four ethylene protons appear as four multiplets (A, B, C, and D in Figure 4) spread over the range δ 2.6–4.2 ppm. The inequivalency of the CH_2 protons could be due to a static conformation[18] of the chelate ring. The separation of the multiplets in a CH_2 moiety is ca. 0.8 ppm. The observed quintet pattern of two multiplets, X(A,C), in Figure 4, could be due to the CH_2 protons (H_e, H_f) adjacent to the amino group. The downfield shift of the other CH_2 protons (H_g, H_i) compared to the shifts for H_e and H_f could be related to the presence of the resonating form $NH_2CH_2CH_2NH{=}C(Me)NH$ in the chelate ring. The close appearance of the H_c and H_d signals also suggests a significant contribution of this resonating form.

Electrochemistry. The electron-transfer behavior of **2** was studied by cyclic voltammetric technique using a platinum working electrode in CH_2Cl_2 containing 0.1 M TBAP. The electrochemical data are given in Table V. The cyclicvoltammograms of **2a** are shown in Figure 5.

Complex **2** undergoes two one-electron redox processes in the potential ranges −0.3 to −0.5 V and +0.9 to +1.0 V vs SCE. Controlled-potential electrolysis done at a potential 200 mV higher than the anodic peak potential (E_{pa}) and 200 mV lower than the cathodic peak potential (E_{pc}) showed that the redox processes occurring at the positive and negative potentials are due to oxidation and reduction of **2**, respectively. The one-electron stoichiometry of the redox couples is obtained from peak current measurements using ferrocene as a standard in under identical experimental conditions. The reversibility of the redox processes can be determined from peak-to-peak separation (ΔE_p) and by measuring the i_{pc}/i_{pa} ratio at various scan rates (v). The current ratio is found to be ca. 1.0 for v = 20–200 mV s^{-1}. The couples involved are given in eq 3, where **2′** denotes the $\{Ru_2(\mu\text{-}O)(\mu\text{-}O_2CAr)_2^{2+}\}$ core of **2**.

Table V. Cyclic Voltammetric Data[a] for $[Ru_2O(O_2CAr)_2\{NH_2CH_2CH_2NHC(Me)NH\}_2(PPh_3)_2](ClO_4)_2$ (**2**) in CH_2Cl_2 Containing 0.1 M TBAP at 20 mV s^{-1}

	$Ru^{III}{}_2 \rightleftharpoons Ru^{II}Ru^{III}$		$Ru^{III}{}_2 \rightleftharpoons Ru^{III}Ru^{IV}$	
complex	$E_{1/2}$, V	ΔE_p, mV	$E_{1/2}$, V	ΔE_p, mV
2a (Ar = C_6H_5)	−0.43	90	+0.93	95
2b (Ar = C_6H_4-*p*-Me)	−0.44	95	+0.92	120
2c (Ar = C_6H_4-*p*-OMe)	−0.45	90	+0.91	100
2d (Ar = C_6H_4-*p*-Cl)	−0.38	110	+0.94	150

[a] Potentials are vs SCE, $\Delta E_p = E_{pa} - E_{pc}$, and $E_{1/2} = (E_{pa} + E_{pc})/2$.

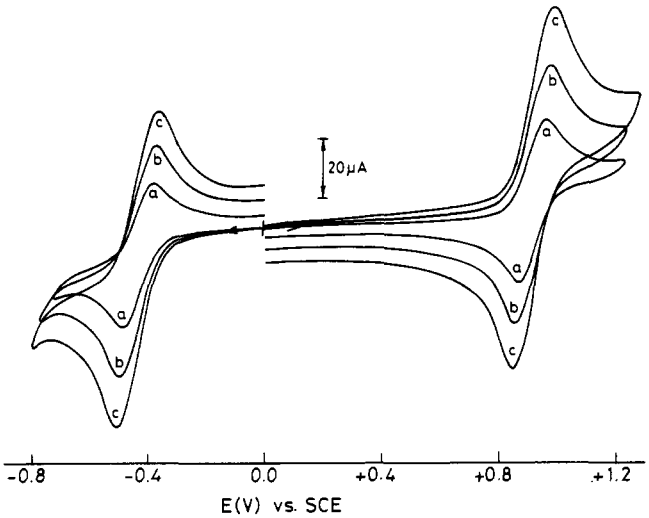

Figure 5. Cyclic voltammograms of $[Ru_2O(O_2CC_6H_5)_2\{NH_2CH_2CH_2NHC(Me)NH\}_2(PPh_3)_2](ClO_4)_2$ (**2a**) in CH_2Cl_2 containing 0.1 M TBAP at scan rates of (a) 20, (b) 50, and (c) 100 mV s^{-1}.

$$\{Ru^{III}Ru^{IV}(\mu\text{-}O)(\mu\text{-}O_2CAr)_2{}^{3+}\} \underset{-e^-}{\overset{+e^-}{\rightleftharpoons}} \underset{\mathbf{2'^{+}}}{} \{Ru^{III}{}_2(\mu\text{-}O)(\mu\text{-}O_2CAr)_2{}^{2+}\} \underset{-e^-}{\overset{+e^-}{\rightleftharpoons}} \underset{\mathbf{2'}}{} \{Ru^{II}Ru^{III}(\mu\text{-}O)(\mu\text{-}O_2CAr)_2{}^{+}\} \underset{\mathbf{2'^{-}}}{} \quad (3)$$

The $E_{1/2}$ values for the **2′** ⇌ **2′**$^+$ couple are much higher than those reported[6,9] for other (μ-oxo)diruthenium(III) complexes.

This could be due to the presence of two facial PPh_3 ligands, which are expected to stabilize the lower oxidation state of the metal compared to hard-base N- and O-donor ligands. The $Ru^{III}{}_2$/$Ru^{II}Ru^{III}$ couple in **2** is found to be quasireversible while the same process in $[Ru_2O(O_2CMe)_2(py)_6]^{2+}$ and $[Ru_2O(O_2CMe)_2(Me_3tacn)_2]^{2+}$ is known[6,9] to be irreversible. Besides the PPh_3 ligands, the amidine functionality of the chelating ligand in **2** enhances the stability of the $Ru^{II}Ru^{III}$ mixed-valence state.

Discussion

The mechanism involved in the formation of the amino-amidine chelate rings in **2** from **1** by the nucleophilic attack of en to the MeCN facial ligands of **1** is an interesting aspect of this study. The amine-amidine chelate formation may take place by either of the two equally probable mechanistic pathways. In pathway a the reaction may proceed through an initial nucleophilic attack of en to the MeCN ligand cis to the μ-oxo ligand followed by a substitution of the trans MeCN ligand by the NH_2 group of en. Pathway b involves an initial substitution of the trans MeCN ligand by en followed by a nucleophilic attack of the free NH_2 group of the η^1-en to the cis MeCN ligand.

In the molecular structure of **1a**, the trans μ-oxo Ru-N bond length of 2.090 (6) Å is longer than the cis μ-oxo Ru-N distance of 2.048 (9) Å.[11] A substitution of the trans MeCN ligand is expected to be more facile than a substitution of the cis ligand. Again, due to the presence of strong interaction in the $\{Ru_2(\mu\text{-}O)^{4+}\}$ moiety, the extent of π-back-bonding from ruthenium to the nitrogen atom of MeCN will be more to the cis ligand than the trans ligand. This is reflected[11] in the C-N bond lengths of **1a**, which shows a longer C-N(cis) bond length compared to the C-N(trans) distance. The PPh_3 facial ligand in **1a** imposing steric constraints on the trans MeCN ligand in presence of two bridging O_2CAr ligands could facilitate a nucleophilic attack on the cis ligand. Structural data[11] on **1** thus clearly suggest a more favorable nucleophilic attack on the cis MeCN ligand than the trans one as is evidenced from the molecular structure and ^1H NMR spectral data of **2**.

Conclusions

A new diruthenium(III) complex, $[Ru_2O(O_2CAr)_2\{NH_2CH_2CH_2NHC(Me)NH\}_2(PPh_3)_2](ClO_4)_2$ (**2**), with an $\{Ru_2(\mu\text{-}O)(\mu\text{-}O_2CAr)_2^{2+}\}$ core and two seven-membered amino-amidine chelate rings, formed by nucleophilic attacks of en to MeCN facial ligands in $[Ru_2O(O_2CAr)_2(MeCN)_4(PPh_3)_2](ClO_4)_2$ (**1**), is isolated and characterized. The X-ray structure of **2c** shows that the nucleophilic attack takes place on the MeCN ligands, which are cis to the μ-oxo ligand in **1**. ^1H NMR spectral studies show a static conformation of the seven-membered chelate rings.

Visible spectral and electrochemical data show the effect of the facial ligands on the electronic structure and the stability of the diruthenium(III) core. The reduction couple $Ru^{III}{}_2/Ru^{II}Ru^{III}$ is found to be quasireversible. In the presence of an asymmetric chelating facial ligand, complex **2** exemplifies the first triply bridged diruthenium(III) complex with three facial sites on each ruthenium occupied by three donor atoms of different σ-donor and π-acceptor abilities, viz., PPh_3, N(amine), and N(amidine).

Acknowledgment. This work was supported by the Council of Scientific and Industrial Research, New Delhi, and the Department of Science and Technology, Government of India.

Registry No. **1a**, 126948-63-8; **1a**$^{3+}$, 136804-65-4; **1b**, 136827-02-6; **1b**$^{3+}$, 136804-66-5; **1c**, 126980-10-7; **1c**$^{3+}$, 136804-67-6; **1d**, 136827-04-8; **2a**, 136804-69-8; **2b**, 136827-06-0; **2c**, 136804-72-3; **2d**, 136804-74-5; en, 107-15-3; MeCN, 75-05-8.

Supplementary Material Available: Details of the crystal structure determination and listings of crystal data, atomic coordinates and isotropic thermal parameters, anisotropic thermal parameters, bond lengths, and bond angles for $[Ru_2O(O_2CC_6H_4\text{-}p\text{-}OMe)_2\{NH_2CH_2CH_2NHC(Me)NH\}_2(PPh_3)_2](ClO_4)_2\cdot CH_2Cl_2\cdot 1.5H_2O$ (16 pages); a table of observed and calculated structure factors (49 pages). Ordering information is given on any current masthead page.

Contribution from the Departments of Inorganic Chemistry and Crystallography of the University of Nijmegen, Toernooiveld, 6525 ED Nijmegen, The Netherlands

Synthesis and Characterization of Copper- and Silver-Containing Platinum-Gold Cluster Compounds. X-ray Crystal Structure of $[Pt(CuCl)(AuPPh_3)_8](NO_3)_2\cdot CH_3OH$

M. F. J. Schoondergang, J. J. Bour, P. P. J. Schlebos, A. W. P. Vermeer, W. P. Bosman, J. M. M. Smits, P. T. Beurskens, and J. J. Steggerda*

Received April 18, 1991

The reactions of CuCl with $[Pt(AuPPh_3)_8]^{2+}$ and $[Pt(CO)(AuPPh_3)_8]^{2+}$ lead to the formation of $[Pt(CuCl)(AuPPh_3)_8]^{2+}$ (**1**) and $[Pt(CO)(CuCl)(AuPPh_3)_8]^{2+}$ (**2**), respectively. On addition of PPh_3 to a reaction mixture containing CuCl and $[Pt(CO)(AuPPh_3)_8]^{2+}$, two CuCl groups are incorporated, yielding $[Pt(CO)(CuCl)_2(AuPPh_3)_7]^+$ (**3**). A cluster with two Ag atoms, $[Pt(CO)(Ag)_2(AuPPh_3)_7]^{3+}$ (**4**), was obtained by treatment of $[Pt(CO)(AuPPh_3)_8]^{2+}$ with 2 equiv of $Ag(PPh_3)NO_3$. The structure of **1** was determined by a single-crystal X-ray analysis. It crystallizes in the triclinic space group $P\bar{1}$ with $Z = 2$, $a = 17.057$ (8) Å, $b = 16.260$ (2) Å, $c = 26.446$ (5) Å, $\alpha = 96.64$ (6)°, $\beta = 97.88$ (2)°, $\gamma = 78.10$ (6)°, and $V = 7080$ (4) Å^3 (Mo Kα radiation). The residuals are $R = 0.060$ and $R_w = 0.069$ for 8071 observed reflections and 460 variables. The probable presence of solvent molecules in the crystal was deduced from this structural analysis. The symmetry of the metal cluster is nearly C_s. The central Pt atom is surrounded by eight Au atoms and one Cu atom. A phosphine is attached to each of the Au atoms, and a Cl atom is attached to the Cu atom. Compared to its parent cluster $[Pt(AuPPh_3)_8]^{2+}$ the cluster has retained its electron count and toroidal geometry. The other PtCu compounds are assumed to contain Pt-Cu bonds as well. They were characterized by elemental analyses and by ^{31}P and ^{195}Pt NMR spectroscopic properties. The ^{195}Pt NMR spectrum of **3** gives evidence for the presence of two Pt-Ag bonds.

Introduction

Since several years, homonuclear gold clusters as well as heteronuclear metal-gold cluster compounds have been studied in our and other laboratories. Several papers and review articles on these clusters were published.[1-9] It is partly due to their potential of being homogeneous catalysts that they have gained such interest. However, up to now only a few have shown catalytic behavior.[10,11] To make metal-gold clusters more interesting from a catalytic point of view, other metal atoms were introduced.

* To whom correspondence should be addressed at the Department of Inorganic Chemistry.

(1) Bott, S. G.; Mingos, D. M. P.; Watson, M. J. *J. Chem. Soc., Chem. Commun.* **1989**, 1192.
(2) Ito, L. N.; Johnson, B. J.; Mueting, A. M.; Pignolet, L. H. *Inorg. Chem.* **1989**, *28*, 2026.
(3) Kanters, R. P. F.; Schlebos, P. P. J.; Bour, J. J.; Steggerda, J. J. *J. Chem. Soc., Chem. Commun.* **1988**, 1634.
(4) Kanters, R. P. F.; Schlebos, P. P. J.; Bour, J. J.; Bosman, W. P.; Smits, J. M. M.; Beurskens, P. T.; Steggerda, J. J. *Inorg. Chem.* **1990**, *29* (2), 324.

0020-1669/91/1330-4704$02.50/0